Title
Dynamics of Micropollutant Adsorption to Polystyrene Surfaces Probed by Angle-Resolved Second Harmonic Scattering

Journal
The Journal of Physical Chemistry C, 123(23)

ISSN
1932-7447

Authors
Cole, William TS
Wei, Haoyun
Nguyen, Son C
et al.

Publication Date
2019-06-13

DOI
10.1021/acs.jpcc.9b01146

Dynamics of Micropollutant Adsorption to Polystyrene Surfaces Probed by Angle- Resolved Second Harmonic Scattering

William T. S. Cole[a], Haoyun Wei[a,b], Son C. Nguyen[c], Charles B. Harris[a], Daniel J. Miller[d*], and Richard J. Saykally[a*]

a) Department of Chemistry, University of California, Berkeley, California 94720, United States

b) State Key Lab of Precision Measurement Technology & Instrument, Department of Precision Instrument, Tsinghua University, Beijing 100084, China

c) Department of Chemistry and Chemical Biology, University of California Merced, 5200 North Lake Road, Merced, California 95343, United States

d) Joint Center for Artificial Photosynthesis, Lawrence Berkeley National Laboratory, Berkeley, California 94720, United States

*Corresponding author emails: danieljmiller@lbl.gov (D.J.M.) and saykally@berkeley.edu (R.J.S.)

Abstract

Angle-resolved second harmonic scattering (SHS) is used to probe the adsorption dynamics of aqueous cationic and anionic dye molecules onto polystyrene surfaces. The adsorptions of Malachite Green (MG) to negatively charged polystyrene and Naphthol Yellow S (NYS) to positively charged polystyrene are both highly favorable, with ΔG_{Ads} values of -10.9 ± 0.2 and -10.27 ± 0.09 kcal/mol, respectively. A competitive displacement methodology was employed to obtain values for the adsorption free energies of various smaller neutral organic molecules, including the important micropollutants ascorbic acid, caffeine, and pentoxifylline. For charged adsorbers, electrostatic interactions appear to significantly contribute to adsorption behavior. However, electrostatic repulsion does not necessarily deter the adsorption of molecules with large uncharged moieties (*e.g.*, surfactants). In these cases, the mechanism of adsorption

is dominated by van der Waals interactions, with surface charge playing a relatively minor role.

Introduction

Understanding the detailed behavior of molecules at aqueous interfaces is of fundamental importance to current research topics, including cloud formation, water purification, ocean chemistry, and catalysis [1,2,11–17,3–10]. The first step towards understanding the behavior of a molecule at an interface is determining the thermodynamics of molecular partitioning between the bulk to the interface. Quantification of, for example, the free energy of adsorption requires a technique that is both surface-specific and specific to the adsorbing molecule [3,5,13,18–21]. Second-order nonlinear spectroscopies exhibit high surface specificity under the dipole approximation and are molecule-specific if a resonant molecular transition exists at either the fundamental or a second-order frequency [21,22]. The two most widely employed second-order techniques, second harmonic generation (SHG) and sum frequency generation (SFG), are normally implemented in reflection geometry [1,2,10]. This geometry

is advantageous when studying liquid-vapor interfaces [1,2,23], and second-order techniques can be extended to liquid-solid interfaces in two ways: First, the surface of a prism in contact with liquid can be probed through the prism; the prism surface in contact with the liquid can be functionalized as desired [24–27]. The second possibility, and that employed herein, is to utilize a scattering geometry on a colloidal sample [11,14,28–31]. Specifically, second harmonic scattering (SHS) has been demonstrated on systems of colloidal polystyrene beads (PSB) [11,19,32], nanoparticles [13,33–36], oil-water droplets [37–41], and biopolymers [14,30,42,43]. By exploiting the constructive interference of dipole radiation from particles with a diameter similar to the relevant light wavelength, surface-sensitive measurements of a colloidal solution are possible [18,22]. Using a dye with a resonantly-enhanced hyperpolarizability at the second harmonic frequency in solution, one can determine the thermodynamics of dye molecule adsorption to the solid surface by SHS [12,32,44]. To extend this technique to molecules without an accessible molecular transition, Eisenthal and coworkers developed a simple displacement methodology, wherein a resonant dye molecule

adsorbed to a solid surface was competitively displaced by the molecule of interest [8]. Eisenthal's technique was later extended by other groups [8,17,28,29]. The resulting decay of the SHS signal is fit to a competitive adsorption model, and the adsorption behavior of the displacing molecule quantified. In addition to characterizing the adsorption thermodynamics of the subject molecule, the molecular orientation can also be determined if the full angle-resolved scattering pattern is recorded with polarization control of the input and output light [12,19,31,45–47]. Several theoretical formalisms have been developed to extract this orientation information, exploiting Mie scattering theory or Rayleigh-Gans-Debye (RGB) scattering theories [19]. Orientation information is particularly valuable for experiments in the vibrational region, wherein vibrational transitions can extract a detailed picture of the chemical structure of an interface [18,37,48,49].

Here, we present a comparative study of the adsorption of two charged dye molecules to both positively and negatively charged polystyrene beads using the method described by Wang *et al.*[17] We also demonstrate that this method can be extended to determine the Gibbs free energy of absorption (ΔG_{Ads}) for non-

resonant, competitor molecules significantly smaller in molecular weight than previously shown by Wang *et al.*[8] We chose the ubiquitous micropollutants caffeine, pentoxifylline, and ascorbic acid, in addition to the surfactants Triton X and cetyl trimethyl ammonium bromide (CTAB) as competitor molecules to demonstrate the range of different molecules that can be studied by this technique. By fitting the SHG data to a competitive adsorption isotherm, we extracted ΔG_{Ads} for the competitors and dyes, as well as the number of adsorption sites on the polystyrene beads (PSB) for the dye molecules. We additionally investigated the differences in interfacial molecular orientation of two resonant dyes, Malachite Green (MG) and Naphthol Yellow S (NYS), for which the structures are shown in Table 1.

Methods

The experiments were performed using a pulsed Ti-Sapphire laser (Spectra Physics Tsunami) operated at 800 nm with a repetition rate of 80 MHz. Each pulse had an average duration of 100 fs and peak energy of ~9 nJ. The input beam was directed through a Faraday isolator (Electo-Optics Technology, Inc.) and a

half-waveplate to control the input polarization, and then directed through an 800 nm bandpass filter to remove any nonlinear frequency components. The input beam was then focused to a beam waist of 50 μm using a microscope objective and directed through the glass sample vial (4mm diameter). The SH output was measured by a collection arm with a maximum angle of acceptance of 2˚, and comprising the following optics in series: an aperture, a focusing optic (f = 38.1 mm), 400 nm bandpass filter, a polarizer, and a final focusing optic (f = 75.6 mm). This arm was attached to a rotating stage with a movement range of 100˚ to either side of the transmission geometry. After the collection arm, SH light was directed into a spectrograph (Acton SpectroPro 2500i) *via* a fiber and into a PMT (Hamamatsu R212) operating in photon counting mode. All reported scans were collected with a counting time of 400 ms and represent the average of 20 separate collections with 2.5˚ steps from -90˚ to 90˚, where 0˚ is defined as the transmission geometry. For the remainder of this report, polarization schemes will be labeled with the input polarization followed by the output polarization (*e.g.*, a polarization of SP corresponds to an input polarization of S and an

output polarization of P). Scans were subjected to background subtraction and normalization by the water signal as outlined in the Supplemental Information (SI).

The water used in all experiments was obtained from a Millipore Milli-Q water purification system (18.2 MΩ•cm at 25 °C, 4 ppb TOC).

Polystyrene samples were purchased from Thermo Fischer Scientific and used as received. According to manufacturer information, the negatively charged PSB was functionalized with sulfate functional groups, which are negatively charged at pH greater than 2. Similarly, the positively charged PSB were functionalized with aliphatic amine functional groups, which are positively charged at pH less than 10. According to the manufacturer, the PSB contained no surfactants and were stabilized in solution by their surface charge. All organic competitor molecules were used as received from the supplier without further purification. Caffeine, pentoxifylline, ascorbic acid, and Triton X were obtained from Sigma Aldrich. CTAB was obtained from Thermo Fischer Scientific.

PSB suspensions were freshly prepared before each experiment to avoid flocculation. Each suspension was prepared by adding the appropriate amount of resonant dye and organic displacer solution and then adding HCl or NaOH solution to achieve the desired solution pH. After pH adjustment, the PSB were added, and the mixture was shaken for 30 seconds. For the generation of the MG and NYS calibration curves, the dye concentration was slowly increased until the SHS intensity began to plateau. For the displacement studies, the dye concentrations were fixed to 1 μM for MG and 10 μM for NYS. These values were chosen because they produced sufficient signal strength, allowing changes in intensity due to competitive adsorption to be easily observed. The initial experiments were performed at different fixed concentrations of MG and the results for the ΔG_{Ads} of the competitor molecules did not change, in agreement with the results of Wang *et al*.[17] Particle radii, measured by dynamic light scattering (DLS) experiments, were 107 ± 2 and 64 ± 1 nm for positively charged PSB (pPSB) and negatively charged PSB (nPSB), respectively, in agreement with reported manufacturer values of 100 ± 10 and 55 ± 10 nm, respectively.

Results

Adsorption of Resonant Dye Molecules

The adsorption of two resonant dye molecules, Malachite Green (MG) and Naphthol Yellow S (NYS), were probed on nPSB and pPSB, respectively. Figure 1 shows the corresponding scattering patterns. There is a significant surface enhancement of the SHS signal relative to the background signals of both the aqueous dyes and the PSB alone. It is important to point out that the dye background signal arises from hyper-Rayleigh scattering, as its scattering pattern peaks at 0˚ (transmission geometry). In contrast, the surface-sensitive signal has a scattering pattern that peaks well away from 0˚ and is a result of the molecular orientation of the dye molecules at the PSB surface [45]. The background contribution was subtracted from the scans to isolate the surface-sensitive signal, and the scans were normalized by the water signal to correct for differences in scattering volume, as has been described in the literature [11].

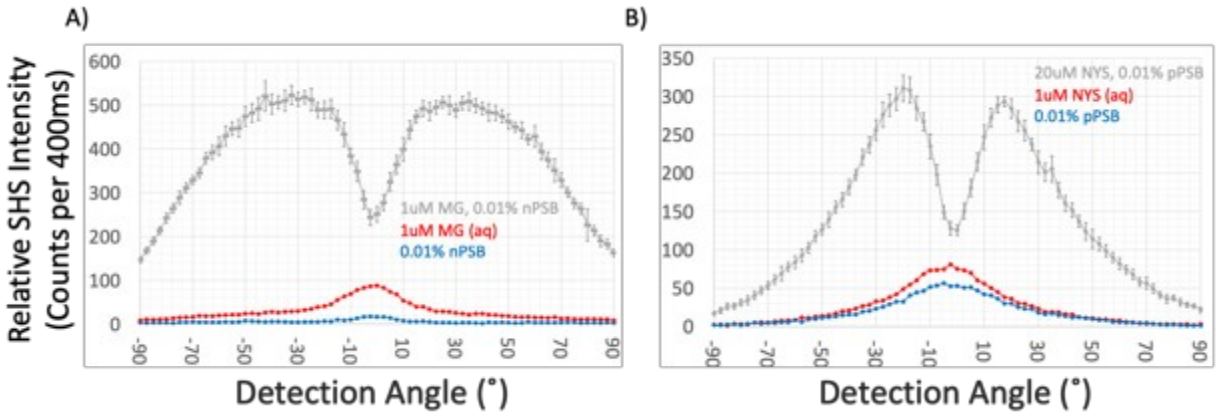

Figure 1: The scattering patterns for malachite green (MG) adsorbed on negative polystyrene (nPSB) (A) and naphthol yellow S (NYS) on positive polystyrene (pPSB) (B). The intensities represent the number of second harmonic photons recorded over a period of 400 ms; each point is the average of 20 measurements at a fixed angle. Error bars are the standard deviation of the arithmetic mean value. The patterns are recorded over an angular range of 180˚ with a resolution of 2.5˚. The data shown have not been subjected to background subtraction or normalization and represent the raw output of the experiment. For both scans, the signal from the dye in solution with the PSB is shown in grey. The background signal from an aqueous solution of the dye is shown in red and the background of the pure PSB in blue.

In order to minimize flocculation, the pH was adjusted to 2 and 4 for pPSB and nPSB suspensions, respectively. The nPSB suspensions were more stable at higher pH, as the threshold PSB concentration at which the particles begin to flocculate is higher for higher pH. However, the resonance of MG shifts away from

the second harmonic frequency of the experiment to longer wavelengths at pH higher than 9 [8,17,27] Additionally, previous studies on MG were performed at pH 4 [8,17], so we also performed our experiments at pH 4 to enable comparison with previously reported data. To determine the free energy of adsorption, the SHS intensity patterns were fit to a modified Langmuir isotherm as described by Wang *et al*.[8,17]

$$I_{SHS} = B + \left[b + a * \theta_D * e^{i\varnothing} \right]^2 (1)$$

where B describes contributions from the constant, non-resonant background, b is the bulk contribution from the PSB sample, a is a fit constant describing the relative signal from the dye molecules at the surface of the bead, θ_D is the fractional coverage of the dye molecule, and Ø is a phase factor corresponding to the interference between the PSB signal and the dye signal. All constants in the above equation are unitless because the SHS intensity is normalized and unitless, as described in the SI. This version of the Langmuir isotherm is the typical first-order model, modified to account for the decrease in bulk dye concentration

due to adsorption to the surface [8]. From Figure 1, it is clear that there is negligible contribution from the PSB particles relative to the surface specific signal. Thus we follow the logic of Wang et al[17] in setting the constant "b" in Equation 1 to zero. We can then also set the phase factor, Ø, to 0 as no interference between the PSB signal and the dye signal is expected.

The fractional coverage, θ_D, of the dye molecule is given by Equation 2:

$$\theta_D = \frac{\left[\left(C_D + N_m^D + \frac{55.5}{K_D}\right) - \left\{\left(C_D + N_m^D + \frac{55.5}{K_D}\right)^2 - 4 C_D N_m^D\right\}^{1/2}\right]}{2 N_m^D} \quad (2)$$

Here C_D is the total concentration of the dye molecule in M, $N_m{}^D$ is the maximum surface number density of the dye molecule in M, and K_D is the equilibrium constant for adsorption in M^{-1}, given by the equilibrium:

$$D + S \Leftrightarrow DS$$

Here D represents a dye molecule, S represents an unoccupied site, and DS is a site occupied by an adsorbed dye molecule. Values of $N_m{}^D$ and K_D can be obtained by fitting SHS signal intensity data to Equations 1 and 2 over a range of dye

concentrations, C_D, for MG and NYS adsorption on nPSB and pPSB, respectively. Calculation of ΔG_{Ads} follows directly from the K_D value using a temperature of 25˚C. The results of these fits are shown in Figure 2. Figure 3 shows the fractional coverage calculated from Equation 2 for both MG and NYS on PSB. All constant values determined by the fits shown in Figure 2 are given in Table 1. The correlation matrices for each fit are shown in the SI.

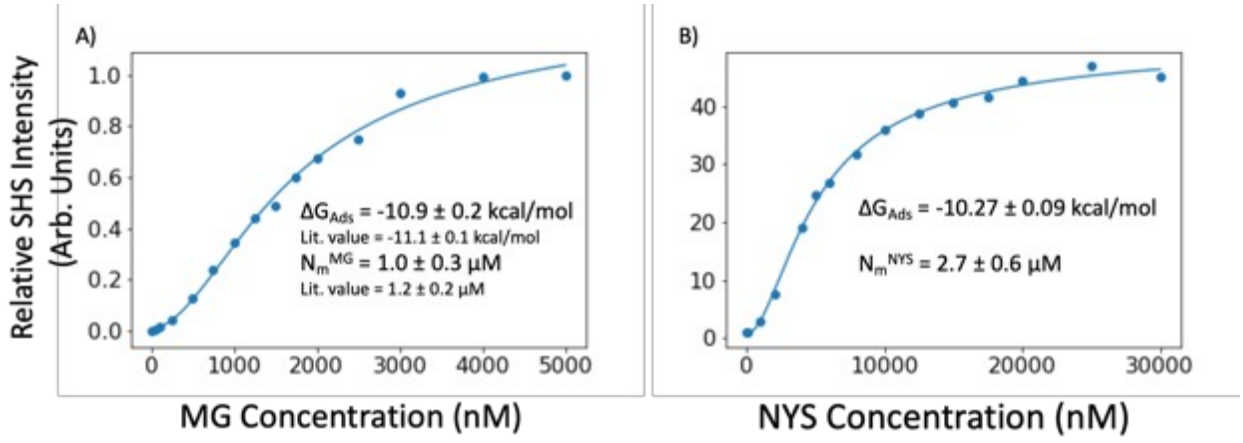

Figure 2: The fits of concentration series of MG adsorbed to (A) nPSB and (B) NYS adsorbed to pPSB to Equation 1. The values of ΔG_{Ads} and N_m^D are shown in the figure insets. Literature values for ΔG_{Ads} and N_m^D in (A) are taken from Wang *et al*.[8] The given uncertainties represent one standard deviation. The data points in Figure 2 represent the average of a sum over the angles of maximum scattering, defined as 30 to 70˚ for MG/nPSB and 15-60˚ for NYS/pPSB. The R^2 value for nPSB is 0.995 and the value for pPSB is 0.998.

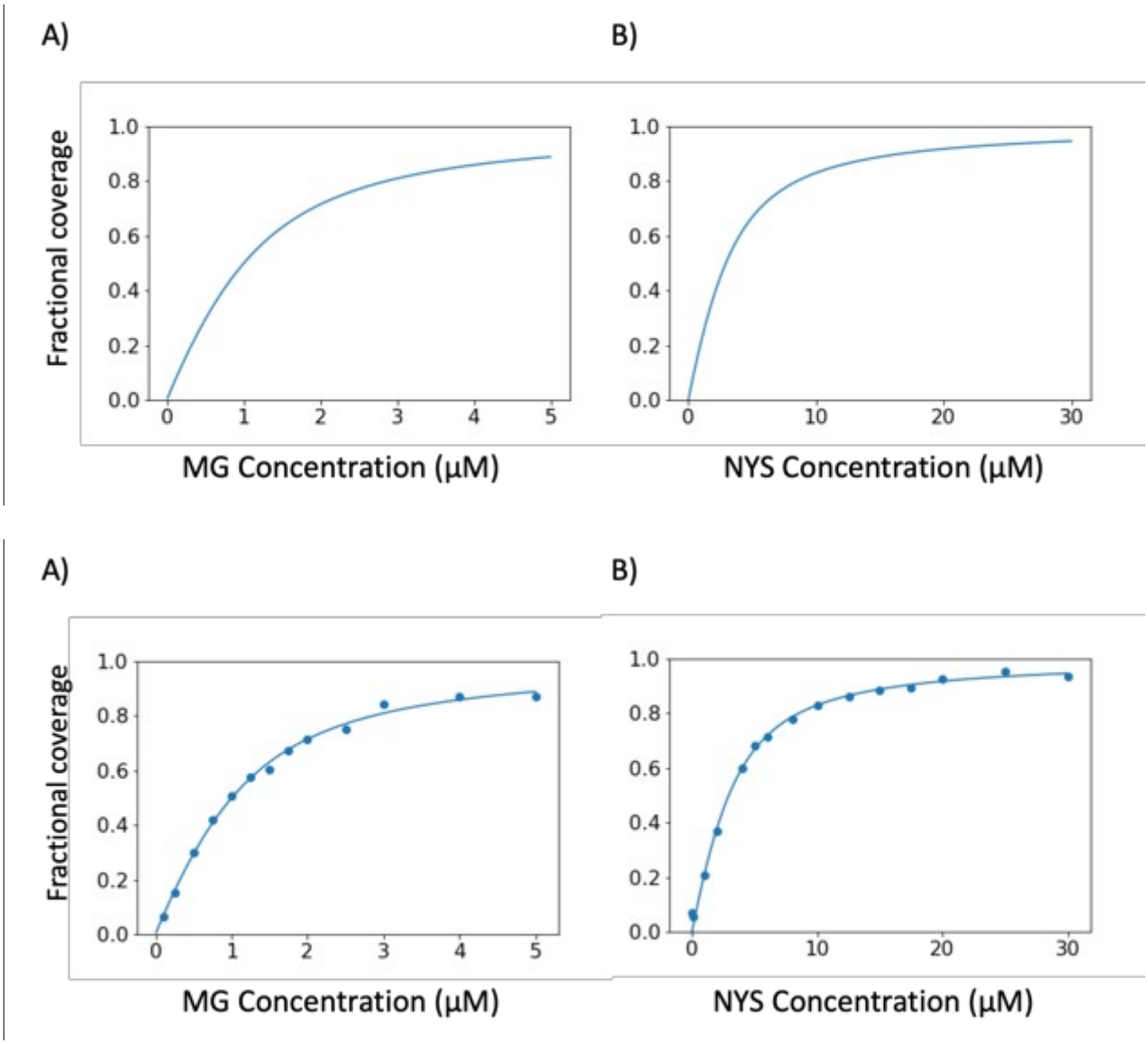

Figure 3: Plots of the fractional coverage of A) MG on nPSB and B) NYS on pPSB. Fractional coverages are calculated from Equation 2 using the constants obtained from the performed fit.

The adsorption of MG to nPSB has been studied previously [8,14,17] and serves as a convenient benchmark for our experimental methodology. We obtained a ΔG_{Ads} value of -11.0 ± 0.2 kcal/mol,

which is comparable to values presented previously in the literature. Wang *et al.* reported the ΔG_{Ads} for MG adsorption to 1μm diameter nPSB to be -11.2 ± 0.1 kcal/mol [8], and later studies reported values in the range -11.1 to -12.7 kcal/mol [12,17,32,43,44]. Schürer and Peukert reported a ΔG_{Ads} value of -11.8 ± 0.5 kcal/mol for polydisperse (controlled mixtures of 0.54 and 1.1 μm diameter) suspensions of nPSB [11]. Additionally, we find similar agreement between our value of 1.0 ± 0.3 μM for N_m^D and a reported value of 1.2 ± 0.2 μM [8].

To our knowledge, the adsorption of NYS to pPSB has not been reported prior to this study. We determined a ΔG_{Ads} value of -10.27 ± 0.09 kcal/mol at pH 2 and a N_m^D value of 2.7 ± 0.6 μM. It is interesting that NYS adsorption to pPSB is similar to MG adsorption to nPSB since NYS is divalent, although direct comparison is difficult due to the difference in surface charge density between the two PSB samples. Nevertheless, determination of ΔG_{Ads} and N_m^D values facilitate displacement studies of non-resonant molecules.

Displacement Studies

To obtain adsorption thermodynamics for non-resonant, competitor molecules, we utilized a displacement methodology first employed by Wang *et al*.[17] to study competitive surfactant adsorption with MG on PSB. For a system in which two molecules compete for surface adsorption, the fractional coverage of the dye molecule becomes:

$$\theta_D = \frac{x}{1+x+y} \quad (3)$$

$$x = \frac{K_D * \left(C_D - N_m^D\right)}{55.5} \quad (4)$$

$$y = \frac{K_C * \left(C_C - N_m^C\right)}{55.5} \quad (5)$$

Here K_C, C_C, and $N_m{}^C$ correspond to the competitor molecule and represent the same physical quantities as their counterparts K_D, C_D, and $N_m{}^D$ (and therefore have the same units). Equation 3 is derived from Equations 5a and 5b in Wang *et al*.[17] Equation 1 in this report is still used to describe the relationship between SHS intensity and the concentrations of the dye molecule and the competitive adsorber.

Two important assumptions of this method are that the surface sites can accommodate either a dye molecule or a competitor, and that all surface sites are chemically equivalent. While these assumptions prevent a detailed characterization of the chemical nature of the surface sites, this method nevertheless provides a route to determination of the relevant adsorption thermodynamics.

Using the determined K_D and N_m^D values for the dye molecule, we performed displacement studies on a variety of competitor molecules over a range of molecular sizes. Table 1 summarizes the results of these studies.

While it is possible to extract an N_m^C value as described by Wang *et al*.[17], relatively high concentrations of the competitor were needed to induce displacement of the dye molecule due to large differences in ΔG_{Ads} values between the dye and competitors. As a result, the numerator in Equation 5 approaches the value C_C and, therefore, N_m^C cannot be fit independently from K_C. We elected to fix N_m^C to the value of N_m^D in order to obtain a meaningful value for K_C. Any error introduced into ΔG_{Ads} from this assumption should be negligible due to the difference in

magnitude between C_C and N_m^C. A previous study by Eckenrode et al[14] showed that by fixing the value of N_m^C, a reasonable estimate of K_C could be obtained. In that study the value of N_m^C was assumed based on the size of the competitor relative to the size of a molecule whose value of N_m^C was directly obtained from the fit. Here we fix the value to that of N_m^D instead of making a similar assumption about relative sizes. Due to the difference in concentrations needed to induce displacement this assumption will only breakdown when the concentration of competitor molecules approaches the value of N_m^D. Given the values of N_m^D in Table 1 of ~1 and ~2 µM we expect the most significant deviations from the model to come from CTAB and TX as those molecules required concentrations on the order of 10 – 100 µM. From inspection of the fits present in the supplemental information of this article, we see that the model appears to accurately describe the displacement behavior of these molecules subject to our choice to fix the value of N_m^C to that of N_m^D.~~; a similar method was used to extract ΔG_{Ads} values for biopolymers by Eisenthal and coworkers [14].~~

Table 1: Collection of fit constants.
Constants for Malachite Green and Naphthol Yellow S were obtained from Equations 1 and 2, while all other constants were obtained from Equations 1and 3-5 as explained in the text. *B* and *a* are fit constants without units, while the units of $N_m{}^D$ and $-\Delta G_{Ads}$ are given in parentheses. The uncertainties provided represent one standard deviation.

Naphthol Yellow S	1.14	0.05

Discussion

Results for the displacement of the dye molecules by caffeine on each PSB surface are shown in Figure 4. Plots for all other displacement experiments are given in the Supplemental Information. The most favorable ΔG_{Ads} values observed were for cationic Malachite Green adsorption to nPSB and anionic NYS adsorption to pPSB. For these molecules that do not have substantial alkyl moieties, electrostatic interactions between the dye and the charged polymer surface may enhance their adsorption relatively to uncharged species. Somewhat surprisingly, ΔG_{Ads} for MG adsorption to nPSB was similar to that for NYS to pPSB (Table 1). NYS is divalent, and it was expected that its adsorption to pPSB could be enhanced relative to the adsorption of monovalent MG to nPSB. A possible explanation would be that the adsorption geometry of NYS to pPSB permits only one of the dye charged groups to interact with the surface charged group. The excellent fit obtained from the first order Langmuir model used herein suggests that a single charged group of NYS interacts with one surface site, although further experiments would be needed to confirm this hypothesis.

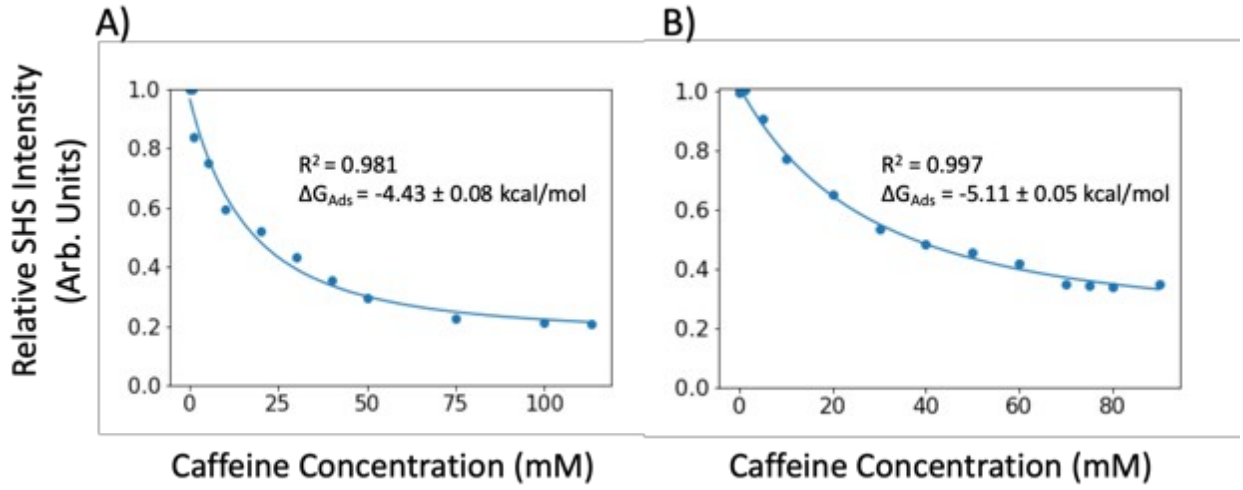

Figure 4: Plots of Caffeine concentration against SHS intensity for A) MG adsorbed o nPSB and B) NYS adsorbed to pPSB. For both plots, the solid, blue line represents the fit performed using equations 1 and 3-5. The insets on each figure give the value for ΔG_{Ads} show in Table 1 and the R^2 value for the fit. Plots for the all other measured competitor molecules can be found in the Supplemental Information.

Given that only 5-10% of the PSB surfaces are charged (according to manufacturer specification), van der Waals interactions are likely to be a significant adsorption driving force. For example, cationic CTAB exhibited a ΔG_{Ads} for adsorption to pPSB that was highly favorable—second only in magnitude to anionic NYS for adsorption to pPSB. While charge-charge interactions likely contribute to the favorable adsorption of NYS to

pPSB, electrostatic repulsion clearly does not deter the adsorption of cationic CTAB to pPSB. Adsorption of CTAB is likely dominated by van der Waals interactions between the long alkyl chain and the large regions of uncharged polystyrene on pPSB. A relatively small effect of the surface charge may be evident in comparing the adsorption of CTAB to the two polymer surfaces, with adsorption of the cationic CTAB to the negatively charged surface being only slightly more favorable than adsorption to the positively charged surface.

Although we expected the adsorption of pentoxifylline to the largely uncharged surface to be more favorable than that of caffeine, these adsorptions were similar. As the only structural difference between these two molecules is the 5-carbon alkyl ketone group on pentoxifylline, this observation may indicate that the present experiment is not suitable for separating the adsorption behavior of very similar molecules. More detailed experiments would be needed to confirm this hypothesis.

Another unexpected observation was the difference in Triton X adsorption to nPSB and pPSB. Triton X is an uncharged surfactant, and we therefore expected similar adsorption behavior

between both PSB surfaces (likely dominated by van der Waals forces between the nonpolar portion of the surfactant and the uncharged surface areas on the polystyrene beads). In our experiments, ΔG_{Ads} was significantly more negative (~1.5 kcal/mol) for Triton X adsorption to nPSB than to pPSB.

These results suggest that the surface sites of the two PSB samples are not equivalent, as evidenced by the different ΔG_{Ads} values obtained for Triton X, caffeine, and pentoxifylline adsorption to the two polymer surfaces. More detailed future studies of the effects of pH and ionic strength are needed to explicitly determine the contribution of surface charge to adsorption to polymer surfaces.

Additionally, while caffeine and pentoxifylline were more likely to adsorb to the positive surface, ascorbic acid adsorbed similarly to both surfaces. As noted in the Results section, the solution pH of the nPSB samples was 4, while that of the pPSB samples was 2. This pH difference is small enough that pKa effects of the competitors are expected to be negligible. Of the studied molecules, only ascorbic acid has a pKa (4.17) near the experimental pH values. Based on the similar ΔG_{Ads} values of

ascorbic acid to pPSB and to nPSB, we conclude that the small pH difference does not significantly affect the adsorption behavior of these molecules.

While other methods, such as UV absorption spectroscopy and adiabatic calorimetry, have been used to probe organic adsorption to polymer surfaces [4,8], those methods suffer from large uncertainties in ΔG_{Ads} (on the order of 1-2 kcal/mol). Our results show that SHS can be effective in probing the adsorption of non-resonant molecules to polymer surfaces, which could enable the study of non-resonant molecules on surfaces other than the PSB presented herein. In addition, the resultant ΔG_{Ads} values have greater precision than those determined with other techniques. For example, the ΔG_{Ads} values measured by Gustafaon *et al*.[4] for various organic molecules to polymer surfaces were 1-2 kcal/mol. Maity *et al.*[7] reported uncertainties in the range of ~8%, whereas the highest uncertainty reported here is 4%. Additionally, interpretation of the scattering pattern of resonant molecules has been shown to provide important details about the molecular orientation of the adsorbate [45]. Studying the

effect of competitive adsorption on molecular orientation could yield important insight into the fundamental adsorption process.

To our knowledge, this study comprises the first use of NYS as a resonant dye for SHS. Previous studies [44] have shown that MG adsorbs to pPSB; however, in our experiments we found the signal from MG adsorbed to pPSB to be dominated by aqueous MG background signal, which led to experimental inconsistency. By utilizing NYS, this problem was mitigated, as the NYS concentrations were below the threshold concentration wherein the second harmonic signal from the solution becomes relevant (see Figure 1).

Conclusions

In summary, we report the extension of a displacement methodology first developed by Wang and coworkers[8,17] for the study of organic surfactant and micropollutant adsorption to polystyrene surfaces. We find that both electrostatic and van der Waals interactions contribute to adsorption to the polymer surface. The polystyrene surfaces employed here had relatively low surface coverage of charged moieties. For charged molecules

without large hydrocarbon regions, electrostatic interactions appeared to contribute to adsorption behavior. For molecules with large hydrocarbon regions (even those containing a charged moiety), adsorption appeared to be dominated by van der Waals interactions. The experimentally determined ΔG_{Ads} values show good agreement with previous studies and excellent precision. The ability to probe non-resonant molecules using SHS suggests that this technique could be extended to studying the adsorption of molecules to a diverse range of surfaces. A more detailed understanding of the contribution of charge-charge interactions could be ascertained through the study of polymer surfaces with greater charge density. Additionally, the effects of pH and ionic strength were not explored and are natural avenues for further experimentation. Application of this technique to the study of practical polymer systems, *e.g.*, those used for water purification membranes, could yield valuable molecular insight about the adsorption process in those materials.

Supplemental Information

The supplemental information attached to this article provides the following: 1) data analysis methodology, 2) the correlation matrices for all fits, and 3) plots of the SHS intensity versus competitor concentration.

Acknowledgments

This work was supported by the Director, Office of Basic Energy Sciences, Office of Science, U.S. Department of Energy (DOE) under Contract No. DE-AC02-05CH11231 through the Chemical Sciences Division of the Lawrence Berkeley National Laboratory (LBNL), by the National Natural Science Foundation of China (NSFC) under Grant No. 61775114, by KAUST under Grant OSR-2016-CRG5-2992, and by CALSOLV (an affiliate of RESOLV) under Fund #56475. This material is based upon work performed at the Joint Center for Artificial Photosynthesis, a DOE Energy Innovation Hub, supported through the Office of Science of the U.S. Department of Energy under Award Number DE-SC000493. The authors would like to thank Mr. Michael Jacobs for performing the DLS experiments.

References

(1) Rizzuto, A. M.; Irgen-Gioro, S.; Eftekhari-Bafrooei, A.; Saykally, R. J. Broadband Deep UV Spectra of Interfacial Aqueous Iodide. *J. Phys. Chem. Lett.* **2016**, *7* (19), 3882–3885.

(2) Mizuno, H.; Rizzuto, A. M.; Saykally, R. J. Charge-Transfer-to-Solvent Spectrum of Thiocyanate at the Air/Water Interface Measured by Broadband Deep Ultraviolet Electronic Sum Frequency Generation Spectroscopy. *J. Phys. Chem. Lett.* **2018**, *9* (16), 4753–4757.

(3) Gonella, G.; Dai, H. L. Second Harmonic Light Scattering from the Surface of Colloidal Objects: Theory and Applications. *Langmuir* **2014**, *30* (10), 2588–2599.

(4) Gustafson, R. L.; Albright, R. L.; Heisler, J.; Lirio, J. A.; Reid, O. T. Adsorption of Organic Species by High Surface Area Styrene-Divinylbenzene Copolymers. *Ind. Eng. Chem. Prod. Res. Dev.* **1968**, *7* (2), 107–115.

(5) Dadap, J. I.; De Aguiar, H. B.; Roke, S. Nonlinear Light Scattering from Clusters and Single Particles. *J. Chem. Phys.* **2009**, *130* (21).

(6) Snyder, S. A.; Adham, S.; Redding, A. M.; Cannon, F. S.; DeCarolis, J.; Oppenheimer, J.; Wert, E. C.; Yoon, Y. Role of Membranes and Activated Carbon in the Removal of Endocrine Disruptors and Pharmaceuticals. *Desalination* **2007**, *202* (1–3), 156–181.

(7) Maity, N.; Payne, G. F.; Ernest, M. V.; Albright, R. L. Caffeine Adsorption from Aqueous Solutions onto Polymeric Sorbents. The Effect of Surface Chemistry on the Adsorptive Affinity and Adsorption Enthalpy. *React. Polym.* **1992**, *17* (3), 273–287.

(8) Wang, H.; Yan, E. C. Y.; Liu, Y.; Eisenthal, K. B. Energetics and Population of Molecules at Microscopic Liquid and Solid Surfaces. *J. Phys. Chem. B* **1998**, *102* (23), 4446–4450.

(9) Miller, D. J.; Dreyer, D. R.; Bielawski, C. W.; Paul, D. R.; Freeman, B. D. Surface Modification of Water Purification Membranes. *Angew. Chemie - Int. Ed.* **2017**, *56* (17), 4662–4711.

(10) McCaffrey, D. L.; Nguyen, S. C.; Cox, S. J.; Weller, H.; Alivisatos, A. P.; Geissler, P. L.; Saykally, R. J. Mechanism of Ion Adsorption to Aqueous Interfaces: Graphene/Water vs.

Air/Water. *Proc. Natl. Acad. Sci.* **2017**, *114* (51), 201702760.

(11) Schürer, B.; Peukert, W. In Situ Surface Characterization of Polydisperse Colloidal Particles by Second Harmonic Generation. *Part. Sci. Technol.* **2010**, *28* (5), 458–471.

(12) Yang, N.; Angerer, W. E.; Yodh, A. G. Angle-Resolved Second-Harmonic Light Scattering from Colloidal Particles. *Phys. Rev. Lett.* **2001**, *87* (10), 1–4.

(13) Gassin, P. M.; Bellini, S.; Zajac, J.; Martin-Gassin, G. Adsorbed Dyes onto Nanoparticles: Large Wavelength Dependence in Second Harmonic Scattering. *J. Phys. Chem. C* **2017**, *121* (27), 14566–14571.

(14) Eckenrode, H. M.; Dai, H. L. Nonlinear Optical Probe of Biopolymer Adsorption on Colloidal Particle Surface: Poly-L-Lysine on Polystyrene Sulfate Microspheres. *Langmuir* **2004**, *20* (21), 9202–9209.

(15) Jen, S. H.; Dai, H. L. Probing Molecules Adsorbed at the Surface of Nanometer Colloidal Particles by Optical Second-Harmonic Generation. *J. Phys. Chem. B* **2006**, *110* (46), 23000–23003.

(16) Wang, H. F.; Troxler, T.; Yeh, A. G.; Dai, H. L. Adsorption at a

Carbon Black Microparticle Surface in Aqueous Colloids Probed by Optical Second-Harmonic Generation. *J. Phys. Chem. C* **2007**, *111* (25), 8708–8715.

(17) Wang, H.; Troxler, T.; Yeh, A. G.; Dai, H. L. In Situ, Nonlinear Optical Probe of Surfactant Adsorption on the Surface of Microparticles in Colloids. *Langmuir* **2000**, *16* (6), 2475–2481.

(18) Roke, S.; Roeterdink, W. G.; Wijnhoven, J. E. G. J.; Petukhov, A. V.; Kleyn, A. W.; Bonn, M. Vibrational Sum Frequency Scattering from a Submicron Suspension. *Phys. Rev. Lett.* **2003**, *91* (25), 1–4.

(19) Wunderlich, S.; Schürer, B.; Sauerbeck, C.; Peukert, W.; Peschel, U. Molecular Mie Model for Second Harmonic Generation and Sum Frequency Generation. *Phys. Rev. B - Condens. Matter Mater. Phys.* **2011**, *84* (23), 1–9.

(20) Gonella, G.; Dai, H. L. Determination of Adsorption Geometry on Spherical Particles from Nonlinear Mie Theory Analysis of Surface Second Harmonic Generation. *Phys. Rev. B - Condens. Matter Mater. Phys.* **2011**, *84* (12), 1–5.

(21) De Beer, A. G. F.; De Aguiar, H. B.; Nijsen, J. F. W.; Roke, S. Detection of Buried Microstructures by Nonlinear Light

Scattering Spectroscopy. *Phys. Rev. Lett.* **2009**, *102* (9), 6–9.

(22) Gonella, G.; Lütgebaucks, C.; De Beer, A. G. F.; Roke, S. Second Harmonic and Sum-Frequency Generation from Aqueous Interfaces Is Modulated by Interference. *J. Phys. Chem. C* **2016**, *120* (17), 9165–9173.

(23) Otten, D. E.; Shaffer, P. R.; Geissler, P. L.; Saykally, R. J. Elucidating the Mechanism of Selective Ion Adsorption to the Liquid Water Surface. *Proc. Natl. Acad. Sci.* **2011**, *109* (8), 701–705.

(24) Konek, C. T.; Musorrafiti, M. J.; Al-Abadleh, H. A.; Bertin, P. A.; Nguyen, S. B. T.; Geiger, F. M. Interfacial Acidities, Charge Densities, Potentials, and Energies of Carboxylic Acid-Functionalized Silica/Water Interfaces Determined by Second Harmonic Generation. *J. Am. Chem. Soc.* **2004**, *126* (38), 11754–11755.

(25) Malin, J. N.; Hayes, P. L.; Geiger, F. M. Interactions of Ca, Zn, and Cd Ions at Buried Solid/Water Interfaces Studied by Second Harmonic Generation. *J. Phys. Chem. C* **2009**, *113* (6), 2041–2052.

(26) Hayes, P. L.; Malin, J. N.; Konek, C. T.; Geiger, F. M.

Interaction of Nitrate, Barium, Strontium and Cadmium Ions with Fused Quartz/Water Interfaces Studied by Second Harmonic Generation. *J. Phys. Chem. A* **2008**, *112* (4), 660–668.

(27) Geiger, F. M. Second Harmonic Generation, Sum Frequency Generation, and $\chi^{(3)}$: Dissecting Environmental Interfaces with a Nonlinear Optical Swiss Army Knife. *Annu. Rev. Phys. Chem.* **2009**, *60* (1), 61–83.

(28) Wang, H.; Yan, E. C. Y.; Borguet, E.; Eisenthal, K. B. Second Harmonic Generation from the Surface of Centrosymmetric Particles in Bulk Solution. *Chem. Phys. Lett.* **1996**, *259* (1–2), 15–20.

(29) Salafsky, J. S.; Eisenthal, K. B. Protein Adsorption at Interfaces Detected by Second Harmonic Generation. *J. Phys. Chem. B* **2000**, *104* (32), 7752–7755.

(30) Liu, J.; Subir, M.; Nguyen, K.; Eisenthal, K. B. Second Harmonie Studies of Ions Crossing Liposome Membranes in Real Time. *J. Phys. Chem. B* **2008**, *112* (48), 15263–15266.

(31) Schürer, B.; Wunderlich, S.; Sauerbeck, C.; Peschel, U.; Peukert, W. Probing Colloidal Interfaces by Angle-Resolved

Second Harmonic Light Scattering. *Phys. Rev. B - Condens. Matter Mater. Phys.* **2010**, *82* (24), 1–4.

(32) Jen, S. H.; Dai, H. L.; Gonella, G. The Effect of Particle Size in Second Harmonic Generation from the Surface of Spherical Colloidal Particles. II: The Nonlinear Rayleigh-Gans-Debye Model. *J. Phys. Chem. C* **2010**, *114* (10), 4302–4308.

(33) Gonella, G.; Gan, W.; Xu, B.; Dai, H. L. The Effect of Composition, Morphology, and Susceptibility on Nonlinear Light Scattering from Metallic and Dielectric Nanoparticles. *J. Phys. Chem. Lett.* **2012**, *3* (19), 2877–2881.

(34) Khebbache, N.; Maurice, A.; Djabi, S.; Russier-Antoine, I.; Jonin, C.; Skipetrov, S. E.; Brevet, P. F. Second-Harmonic Scattering from Metallic Nanoparticles in a Random Medium. *ACS Photonics* **2017**, *4* (2), 262–267.

(35) Gan, W.; Xu, B.; Dai, H. L. Activation of Thiols at a Silver Nanoparticle Surface. *Angew. Chemie - Int. Ed.* **2011**, *50* (29), 6622–6625.

(36) Haber, L. H.; Kwok, S. J. J.; Semeraro, M.; Eisenthal, K. B. Probing the Colloidal Gold Nanoparticle/Aqueous Interface with Second Harmonic Generation. *Chem. Phys. Lett.* **2011**,

507 (1–3), 11–14.

(37) Vaécha, R.; Rick, S. W.; Jungwirth, P.; De Beer, A. G. F.; De Aguiar, H. B.; Samson, J. S.; Roke, S. The Orientation and Charge of Water at the Hydrophobic Oil Droplet - Water Interface. *J. Am. Chem. Soc.* **2011**, *133* (26), 10204–10210.

(38) De Aguiar, H. B.; De Beer, A. G. F.; Strader, M. L.; Roke, S. The Interfacial Tension of Nanoscopic Oil Droplets in Water Is Hardly Affected by SDS Surfactant. *J. Am. Chem. Soc.* **2010**, *132* (7), 2122–2123.

(39) De Aguiar, H. B.; Strader, M. L.; De Beer, A. G. F.; Roke, S. Surface Structure of Sodium Dodecyl Sulfate Surfactant and Oil at the Oil-in-Water Droplet Liquid/Liquid Interface: A Manifestation of a Nonequilibrium Surface State. *J. Phys. Chem. B* **2011**, *115* (12), 2970–2978.

(40) Zhong, Q.; Baronavski, A. P.; Owrutsky, J. C. Reorientation and Vibrational Energy Relaxation of Pseudohalide Ions Confined in Reverse Micelle Water Pools. *J. Chem. Phys.* **2003**, *119* (17), 9171–9177.

(41) Zhong, Q.; Steinhurst, D. A.; Carpenter, E. E.; Owrutsky, J. C. Fourier Transform Infrared Spectroscopy of Azide Ion in

Reverse Micelles. *Langmuir* **2002**, *18* (20), 7401–7408.

(42) Srivastava, A.; Eisenthal, K. B. Kinetics of Molecular Transport across a Liposome Bilayer. *Chem. Phys. Lett.* **1998**, *292* (3), 345–351.

(43) Liu, Y.; Yan, E. C. Y.; Eisenthal, K. B. Effects of Bilayer Surface Charge Density on Molecular Adsorption and Transport across Liposome Bilayers. *Biophys. J.* **2001**, *80* (2), 1004–1012.

(44) Eckenrode, H. M.; Jen, S. H.; Han, J.; Yeh, A. G.; Dai, H. L. Adsorption of a Cationic Dye Molecule on Polystyrene Microspheres in Colloids: Effect of Surface Charge and Composition Probed by Second Harmonic Generation. *J. Phys. Chem. B* **2005**, *109* (10), 4646–4653.

(45) De Beer, A. G. F.; Roke, S. Obtaining Molecular Orientation from Second Harmonic and Sum Frequency Scattering Experiments in Water: Angular Distribution and Polarization Dependence. *J. Chem. Phys.* **2010**, *132* (23).

(46) Chen, Y.; Okur, H. I.; Liang, C.; Roke, S. Orientational Ordering of Water in Extended Hydration Shells of Cations Is Ion-Specific and Is Correlated Directly with Viscosity and Hydration Free Energy. *Phys. Chem. Chem. Phys.* **2017**, *19*

(36), 24678–24688.

(47) Ong, S.; Zhao, X.; Eisenthal, K. B. Polarization of Water Molecules at a Charged Interface: Second Harmonic Studies of the Silica/Water Interface. *Chem. Phys. Lett.* **1992**, *191* (3–4), 327–335.

(48) Okur, H. I.; Chen, Y.; Smolentsev, N.; Zdrali, E.; Roke, S. Interfacial Structure and Hydration of 3D Lipid Monolayers in Aqueous Solution. *J. Phys. Chem. B* **2017**, *121* (13), 2808–2813.

(49) Yang, N.; Angerer, W. E.; Yodh, A. G. Second-Harmonic Microscopy of Single Micrometer-Size Particles on a Substrate. *Phys. Rev. A - At. Mol. Opt. Phys.* **2001**, *64* (4), 4.